High-efficiency 5000 lines/mm multilayer-coated blazed grating for extreme ultraviolet wavelengths

Dmitriy L. Voronov,[1,*] Minseung Ahn,[2] Erik H. Anderson,[1] Rossana Cambie,[1] Chih-Hao Chang,[2] Eric M. Gullikson,[1] Ralf K. Heilmann,[2] Farhad Salmassi,[1] Mark L. Schattenburg,[2] Tony Warwick,[1] Valeriy V. Yashchuk,[1] Lucas Zipp,[1] and Howard A. Padmore[1]

[1]*Lawrence Berkeley National Laboratory, 1 Cyclotron Road, Berkeley, California 94720, USA*

[2]*Space Nanotechnology Laboratory, Massachusetts Institute of Technology, 70 Vassar Street, Cambridge, Massachusetts 02139, USA*

**Corresponding author: dlvoronov@lbl.gov*

Received May 10, 2010; revised July 2, 2010; accepted July 3, 2010; posted July 13, 2010 (Doc. ID 126812); published July 29, 2010

Volume x-ray gratings consisting of a multilayer coating deposited on a blazed substrate can diffract with very high efficiency, even in high orders if diffraction conditions in-plane (grating) and out-of-plane (Bragg multilayer) are met simultaneously. This remarkable property, however, depends critically on the ability to create a structure with near atomic perfection. In this Letter we report on a method to produce these structures. We report measurements that show, for a 5000 l/mm grating diffracting in the third order, a diffraction efficiency of 37.6% at a wavelength of 13.6 nm. This work now shows a direct route to achieving high diffraction efficiency in high order at wavelengths throughout the soft x-ray energy range. © 2010 Optical Society of America

OCIS codes: 050.1950, 120.6660, 340.7480, 230.4170, 310.1860.

Multilayer (ML)-coated blazed gratings seem to be the best choice [1] for many high-resolution soft x-ray spectroscopy techniques, such as resonance inelastic x-ray scattering [2], that require high spectral resolution ($10^4 - 10^6$) combined with high efficiency. Such gratings should have a high groove density and operate in a high diffraction order, because resolution depends directly on the m/d ratio (for a fixed grating size), where m is a blazed order and d is the grating period. Moreover, high dispersion of the gratings with a large effective groove density allows the use of larger slits, providing more light through a spectrograph or monochromator. A ML coating provides high grating efficiency and moves the spectrometer design away from the grazing incidence. This reduces problems of geometric aberration and increases the grating acceptance, thus increasing throughput while decreasing the dimensions of the whole system [3].

To realize the advantages of ML blazed gratings in the extreme ultraviolet (EUV) and soft x-ray range, sawtooth substrates of very high quality are required. The smoothness of the facet surface and the profile of the grooves are the main concerns [4]. The best EUV blazed gratings have been fabricated with interference lithography combined with ion-beam etching [5,6], or gray-scale e-beam lithography [7]. Efficiency of 41% has been obtained in first-order diffraction at the wavelength of 12.5 nm with a 1000 groove/mm grating [7]. A denser 2400 groove/mm grating has demonstrated efficiency in the second diffraction order of 36.2% at a wavelength of 15.79 nm [6], and 29.9% was achieved for a second-order grating with the groove density of 3000 groove/mm [5]. These spectacular achievements show that the measured efficiency of the gratings is nevertheless significantly below the theoretical prediction, and technological challenges increase significantly for high groove density and high orders.

We believe that wet anisotropic etch of silicon is the most promising technique for high-resolution grating fabrication [8]. The process can provide both a triangular groove profile and an atomically smooth surface of the blazed facets, due to crystal lattice perfection and the high anisotropy of the etch. This technique has been successfully applied to fabricate hard x-ray blazed gratings operating at grazing incidence [9]. A first attempt to fabricate a ML-coated blazed grating for soft x rays showed that thorough optimization of the etch process is necessary to realize the advantages of the anisotropic etch approach [10]. Here we describe the fabrication process of a EUV blazed grating with effective groove density, m/d, of 15,000 lines/mm, and present measurements of efficiency of the grating coated with a Mo/Si ML.

The sawtooth gratings were fabricated by KOH etching of asymmetrically cut silicon single crystals. Float zone (111) silicon wafers with a 6° miscut toward the [112] direction were used. After low-stress CVD silicon nitride deposition, antireflection coating and photoresist spinning the wafers were patterned with scanning beam interference lithography [11]. Then the 200 nm period pattern was transferred to the nitride layer with an O_2 and CF_4 reactive ion etch. The wet etch of the samples was performed in 20% KOH solution stirred intensively at room temperature.

The scanning electron microscope (SEM) image of the gratings after the etching and nitride mask strip is shown in Fig. 1(a). The grating grooves consist of 6° tilted blazed facets with silicon nubs, which are also shaped with $\{111\}$ sidewalls. The surface of the blazed facets consists of atomically smooth (111) terraces and atomic steps [Fig. 2(a)]. This kind of morphology is inherent for anisotropic etch because of the step-flow mechanism of the etch process [12]. Net roughness of the surface is defined by step density, which in turn depends on anisotropy of the reaction. Atomic force microscopy (AFM) measurements showed roughness below 0.3 nm rms measured over a 1 μm × 1 μm area. This is close to the

 © 2010 Optical Society of America

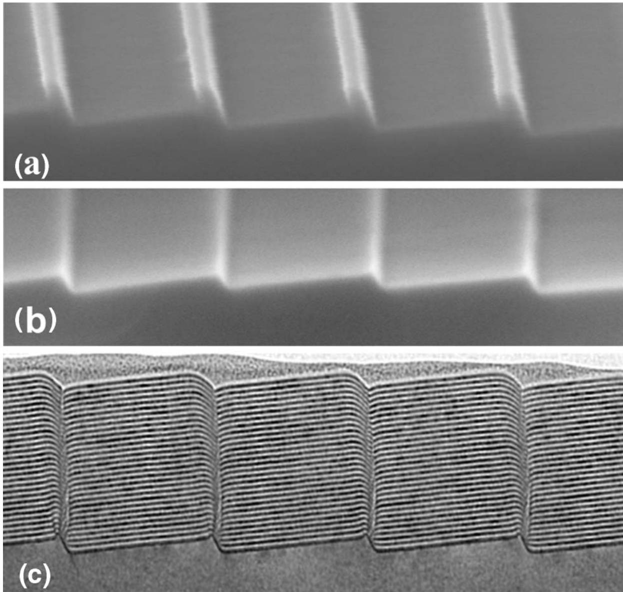

Fig. 1. SEM images of the 200 nm grating (a) after KOH etch and nitride mask removal, (b) after nub removal, and (c) cross-section TEM image of the grating coated with the Mo/Si ML.

silicon lattice spacing in the (111) direction, and, indeed, many of the AFM images showed clear evidence of (111) terraces and steps.

The silicon nubs remaining after the etch step must be removed before ML deposition, otherwise they can cause significant perturbation of the ML structure [13]. We used chemical oxidation of silicon with piranha solution ($H_2SO_4 + H_2O_2$) followed by an oxide etch with HF as a nub removal process. Each oxidation/oxide etch cycle

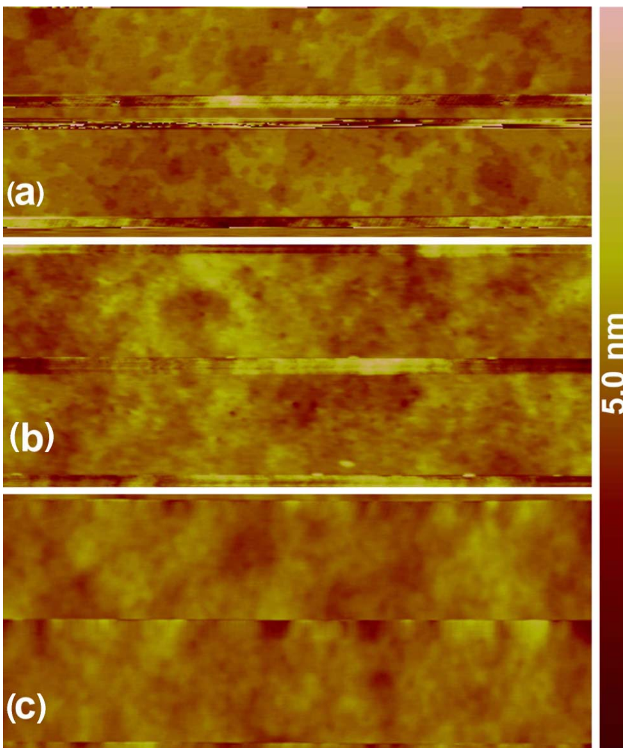

Fig. 2. (Color online) Morphology of the groove surface of the blazed gratings after (a) KOH etching, (b) nub removal, and (c) ML deposition.

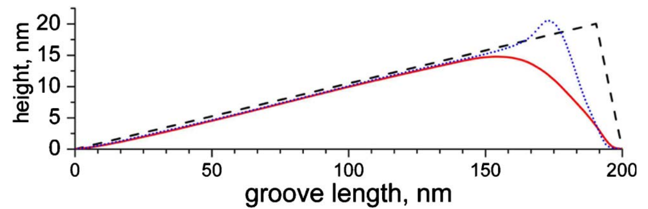

Fig. 3. (Color online) Ideal profile of a silicon blazed grating (dashed curve) and averaged profiles measured with AFM for the grating before (dotted curve) and after (solid curve) ML deposition.

removes an approximately 0.5-nm-thick silicon layer. In total, 26 cycles were applied in order to remove the 25-nm-wide nubs and to get the groove profile close to a triangle (Fig. 3). The nub removal process results in a slight increase of a high spatial frequency component of surface roughness up to 0.34 nm rms [Fig. 2(b)], which is easily smoothed out to 0.3 nm rms by the ML deposition step that follows [Fig. 2(c)].

The ML, composed of 30 Mo/Si bilayers, was deposited onto the blazed grating substrates by dc-magnetron sputtering. The ML period was targeted to 7.2 nm in order to bring the third diffraction order of the grating to the blaze condition and at the same time satisfy the first-order Bragg condition for the ML. The groove profile of the grating changes significantly during the course of the deposition. Figure 1(c) shows a cross-section TEM image of the ML-coated grating, and Fig. 3 shows the AFM measurements of the average groove profile before and after deposition of the ML. Coating causes the surface of the blazed facets to become slightly convex and the apexes of the triangle groove to become rounded significantly.

The diffraction efficiency of the ML-coated blazed grating was measured with an Advanced Light Source beamline 6.3.2 two-axis diffractometer [14]. The incident angle was set to 11° from the grating surface normal, and an angular resolution of 0.12° was used for the detector axis. The detector scans over the diffraction angle were performed at the wavelengths between 12.7 nm and 15.0 nm with an increment of 0.1 nm. The data were normalized to the direct beam measured over the wavelength range.

Figure 4 shows the diffraction from the Mo/Si-30 coated grating at the wavelength of 13.6 nm. The blazed third diffraction order demonstrates efficiency as high as

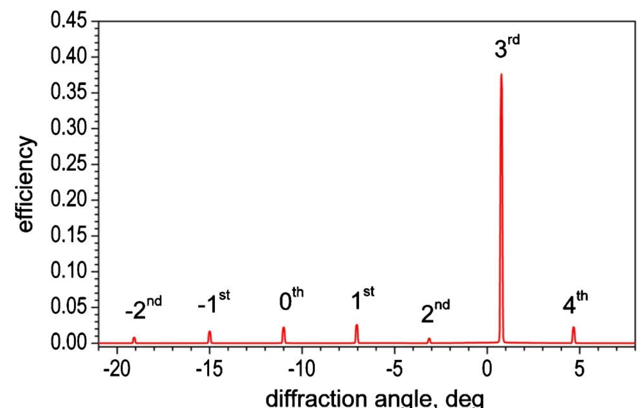

Fig. 4. (Color online) Diffraction from the Mo/Si-30 ML-coated grating measured at an incidence angle of 11° and wavelength of 13.6 nm.

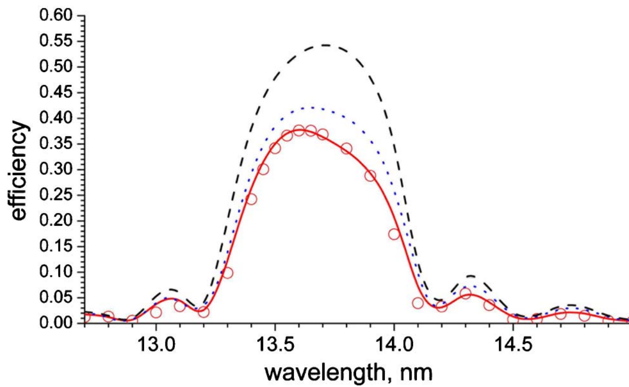

Fig. 5. (Color online) Experimental (circles) and simulated dependence of efficiency of the third order on the wavelength. The simulation was performed for an ideal groove profile (dashed curve), and experimental profiles before (dotted curve) and after (solid curve) deposition of the Mo/Si-30 ML. The interface width of 0.9 nm rms was taken into account for all the simulations.

37.6%, and the nonblazed orders are well suppressed. Figure 5 shows experimental and simulated efficiency of the third order versus the wavelength. Simulations were performed with a commercial code based on the rigorous approach of boundary integral equations [15]. These simulations reveal that the experimental substrate groove profile (dashed curve) provides a lower grating efficiency than the ideal one. In addition, smoothing of the groove profile by the ML has a negative impact on grating efficiency. The grating efficiency could be higher if the grating profile was preserved during the ML deposition. The rounding is caused by both the geometry of the magnetron sputtering used for ML deposition as well as resputtering processes and surface atom mobility, which results in smoothing high spatial frequency features of the surface topography. One can expect that use of ML deposition with a collimated atomic flux would reduce rounding significantly and improve the grating efficiency.

In summary, we developed a process for fabrication of high quality EUV diffraction gratings with a groove density of 5000 lines/mm. Substrate blazed gratings were made by scanning beam interference lithography and anisotropic KOH etching of silicon. The optimized anisotropic etching provides excellent control of the slope of blazed facets, high smoothness of the facet surface, and very short antiblazed facets. A new nub removal step provides a triangular substrate groove profile, which is close to the ideal one. The grating coated with Mo/Si-30 ML demonstrated an efficiency of 37.6% in the third diffraction order at 13.6 nm wavelength. The triangular substrate groove profile suffers some smoothing during the ML deposition with dc-magnetron sputtering. It may be that collimated deposition of the ML could address this issue. Fabrication of near atomically perfect blazed substrates opens up the prospect of highly efficient high-order diffraction gratings for the whole of the soft x-ray energy region, provided the ML deposition process will be improved. Applications include ultra-high-resolution spectroscopy as well as pulse compression of chirped x-ray beams.

This work was supported by the United States Department of Energy (DOE) under contract DE-AC02-05CH11231.

References

1. D. L. Voronov, R. Cambie, R. M. Feshchenko, E. Gullikson, H. A. Padmore, A. V. Vinogradov, and V. V. Yashchuk, Proc. SPIE **6705**, 67050E (2007).
2. *Proceedings of the Workshop on Soft X-Ray Science in the Next Millennium: The Future of Photon-In/Photon-Out Experiments* (2000), http://www.phys.utk.edu/WPWebSite/ewp_workshop_X-Ray_Report.pdf.
3. T. Warwick, H. A. Padmore, D. Voronov, and V. Yashchuk, presented at the Tenth International Conference on Synchrotron Radiation Instrumentation Melbourne, Victoria, Australia, 27 Sept.–2 Oct. 2009.
4. J. C. Rife, T. W. Barbee, Jr., W. R. Hunter, and R. G. Cruddace, Phys. Scr. **41**, 418 (1990).
5. M. P. Kowalski, R. G. Cruddace, K. F. Heidemann, R. Lenke, H. Kierey, T. W. Barbee, Jr., and W. R. Hunter, Opt. Lett. **29**, 2914 (2004).
6. H. Lin, L. Zhang, L. Li, Ch. Jin, H. Zhou, and T. Huo, Opt. Lett. **33**, 485 (2008).
7. P. P. Naulleau, J. A. Liddle, E. H. Anderson, E. M. Gullikson, P. Mirkarimi, F. Salmassi, and E. Spiller, Opt. Commun. **229**, 109 (2004).
8. P. Philippe, S. Valette, O. Mata Mendez, and D. Maystre, Appl. Opt. **24**, 1006 (1985).
9. A. E. Franke, M. L. Schattenburg, E. M. Gullikson, J. Cottam, S. M. Kahn, and A. Rasmussen, J. Vac. Sci. Technol. B **15**, 2940 (1997).
10. J. H. Underwood, C. Kh. Malek, E. M. Gullikson, and M. Krumrey, Rev. Sci. Instrum. **66**, 2147 (1995).
11. R. K. Heilmann, C. G. Chen, P. T. Konkola, and M. L. Schattenburg, Nanotechnology **15**, S504 (2004).
12. R. A. Wind and M. A. Hines, Surf. Sci. **460**, 21 (2000).
13. D. L. Voronov, R. Cambie, E. M. Gullikson, V. V. Yashchuk, H. A. Padmore, Yu. P. Pershin, A. G. Ponomarenko, and V. V. Kondratenko, Proc. SPIE **7077**, 707708 (2008).
14. http://www-cxro.lbl.gov/beamlines/6.3.2.
15. http://www.pcgrate.com.